Molecular Architecture of the Ankyrin SOCS Box Family of Cul5-Dependent E3 Ubiquitin Ligases

João R.C. Muniz[1], Kunde Guo[1], Nadia J. Kershaw[2], Vikram Ayinampudi[1], Frank von Delft[1], Jeffrey J. Babon[2] and Alex N. Bullock[1]

*1 - **Structural Genomics Consortium,** University of Oxford, Old Road Campus Research Building, Roosevelt Drive, Oxford OX3 7DQ, United Kingdom*

*2 - **Walter and Eliza Hall Institute of Medical Research and Department of Medical Biology,** University of Melbourne, Parkville, Victoria, Australia*

Correspondence to Alex N. Bullock: *alex.bullock@sgc.ox.ac.uk*
http://dx.doi.org/10.1016/j.jmb.2013.06.015
Edited by M. Guss

Abstract

Multi-subunit Cullin–RING E3 ligases often use repeat domain proteins as substrate-specific adaptors. Structures of these macromolecular assemblies are determined for the F-box-containing leucine-rich repeat and WD40 repeat families, but not for the suppressor of cytokine signaling (SOCS)-box-containing ankyrin repeat proteins (ASB1–18), which assemble with Elongins B and C and Cul5. We determined the crystal structures of the ternary complex of ASB9–Elongin B/C as well as the interacting N-terminal domain of Cul5 and used structural comparisons to establish a model for the complete Cul5-based E3 ligase. The structures reveal a distinct architecture of the ASB9 complex that positions the ankyrin domain coaxial to the SOCS box–Elongin B/C complex and perpendicular to other repeat protein complexes. This alternative architecture appears favorable to present the ankyrin domain substrate-binding site to the E2-ubiquitin, while also providing spacing suitable for bulky ASB9 substrates, such as the creatine kinases. The presented Cul5 structure also differs from previous models and deviates from other Cullins via a rigid-body rotation between Cullin repeats. This work highlights the adaptability of repeat domain proteins as scaffolds in substrate recognition and lays the foundation for future structure–function studies of this important E3 family.

Introduction

Lysine ubiquitylation regulates proteasome-dependent protein degradation, as well as changes in protein localization and activity [1,2]. Ubiquitin is first loaded by an E1 ubiquitin-activating enzyme onto an E2-ubiquitin-conjugating enzyme. E3 ubiquitin ligases subsequently recruit the charged E2 as well as substrate to catalyze the transfer of ubiquitin onto the ε-amine of a target lysine. Over 600 human E3 ligases are identified, offering a rich variety of structures to accommodate substrates of varying shapes and sizes. Among the most complex E3s are the Cullin–RING E3 ligases, which adopt a modular architecture that combines separate substrate-binding and catalytic subunits [3,4]. The Cullin subunit (Cul1–5 or Cul7) binds specific substrate-recognition proteins and their adaptors through its N-terminal domain (NTD), whereas the C-terminal domain (CTD) binds a RING protein (Rbx1 or Rbx2), which in turn recruits the E2-ubiquitin conjugate. The substrate and ubiquitin are brought into juxtaposition for ligation upon neddylation of the Cullin CTD [5,6].

The best characterized complexes are of the SCF (Skp1–Cul1–F-box) type, which commonly include the WD40 repeat or leucine-rich repeat domain, for which a complete crystal structure is known [7]. In these E3s, the F-box domain of the substrate-recognition protein binds the adaptor Skp1 to form a bipartite interface with Cul1. Similarly, suppressor of cytokine signaling (SOCS)-box-containing proteins form SCF-like E3 ligases by assembly with the adaptor Elongin C, its partner Elongin B, and either Cul2 or Cul5 [8,9]. Although first identified in the SOCS SH2 family, the SOCS box is now recognized in over 60 human proteins, including proteins containing ankyrin repeats, WD40 repeats, SPRY

domains, RAB GTPases, and the von Hippel–Lindau tumor suppressor protein [10–13].

The ankyrin SOCS box (ASB) family comprising ASB1–18 represents the largest class of SOCS box proteins but remains relatively poorly characterized. ASB family proteins contain an N-terminal ankyrin repeat domain for substrate recognition and a C-terminal SOCS box for assembly with Elongin B/C, Cul5, and Rbx2 [13–15]. ASB2 appears suppressive for the growth of myeloid leukemia cells [14] and contributes to hematopoietic differentiation through the destruction of the mixed-lineage leukemia protein [16], as well as filamins A and B [17]. Similarly, ASB9 negatively regulates cell growth by ubiquitylation and destruction of ubiquitous mitochondrial creatine kinase [18] and creatine kinase B [19]. Increased expression of ASB9 correlates with improved prognosis in colorectal cancer [20]. ASB3 and ASB4 are identified as E3 ligases for tumor necrosis factor receptor II [21] and insulin receptor substrate 4 [22], respectively. Finally, zebrafish d-ASB11 degrades the Notch ligand DeltaA to control Notch signaling and neurogenesis [23,24].

To date, the only available ASB family structure is that of the truncated ASB9-2 isoform, which lacks the SOCS box and E3 activity [25]. To establish how the ankyrin domain folds stably with the SOCS box to facilitate E3 function, we determined the crystal structures of the ternary ASB9–Elongin B/C complex as well as the first structure of the Cul5 NTD. These data show that the SOCS box of ASB9 contains an insertion within its classical three-helix architecture that contacts the ankyrin repeats of ASB9 to induce a specific and stable orientation between the two domains that differs from previous SCF-type structures. Likewise, current models of the Cul5 subunit are revised by changes to the Cullin repeat alignments and internal domain rotations. This work reveals for the first time the distinct molecular architecture of the ASB family and further highlights the structural diversity that helps the Cullin–RING E3 ligases to capture their many important targets.

Results

Structure of the ASB9–Elongin B/C complex

Human ASB proteins were co-purified with Elongins B and C and screened for crystallization to define the structural basis for their assembly. Viable crystals were obtained in space group $P2_122_1$ using a complex containing residues 35 to 294 of human ASB9. The structure of the ternary complex was

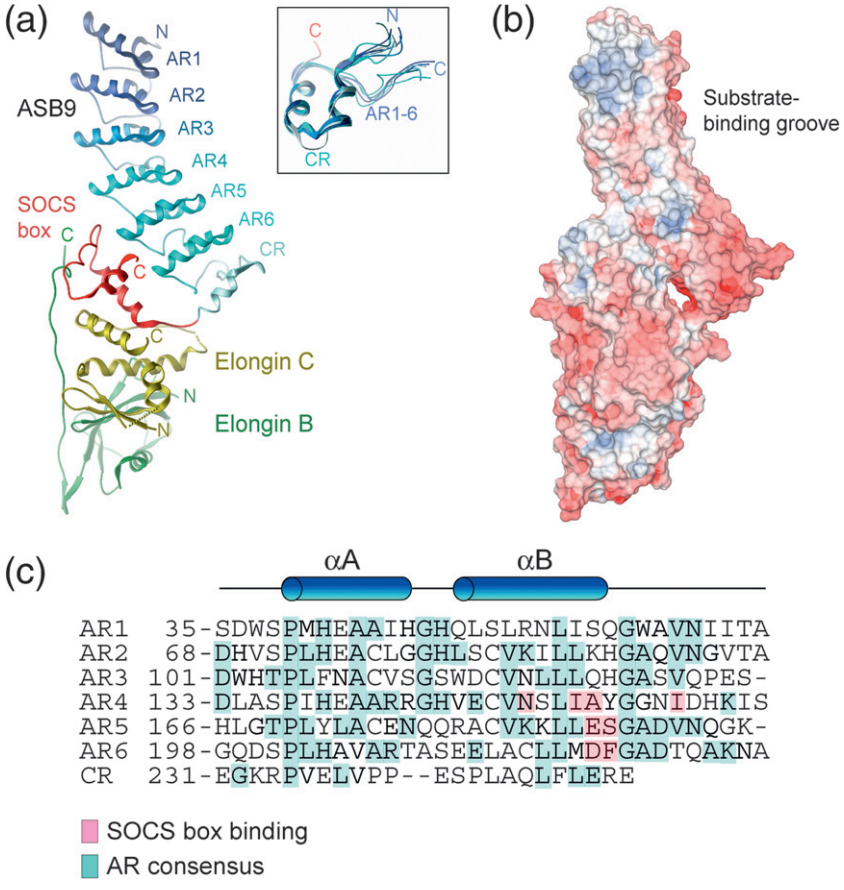

Fig. 1. Structure of the ASB9–Elongin B/C complex. (a) Ribbon diagram of the ternary complex colored by domain. Inset shows the superposition of the consensus ankyrin repeats (AR1–6) and the capping repeat (CR), which precedes the C-terminal SOCS box (red C-terminus). (b) A molecular surface representation of the complex identifies a solvent channel between the capping repeat and the SOCS box. The surface is colored by electrostatic surface potential on a scale between −10 kT/e (red) and +10 kT/e (blue). (c) Structure-based sequence alignment of ankyrin repeats highlighting residues involved in SOCS box interaction (pink) and those that conform to the ankyrin repeat consensus (cyan) [26,27].

Table 1. Summary of data collection and refinement statistics

	ASB9–Elongin B/C	$Cul5^{NTD}_{native}$	$Cul5^{NTD}_{SeMet}$
Data collection			
Space group	$P2_122_1$	$P2_12_12_1$	$P2_12_12_1$
Wavelength (Å)	0.980	0.980	0.980
Unit cell dimensions (Å): *a*, *b*, *c* (α = β = γ = 90°)	102.86, 110.74, 113.41	30.18, 64.50, 197.54	30.11, 64.35, 197.50
Resolution range (Å)	50.47–2.58	33.69–2.05	65.83–2.27
Number of unique reflections	41,297 (5914)	25,290 (3681)	18,727 (2657)
R_{meas} (%)	10.6 (83.9)	14.5 (80.9)	12.4 (46.7)
$\langle I \rangle / \langle \sigma I^* \rangle$	10.7 (2.1)	7.4 (2.0)	13.6 (4.4)
Completeness (%)	99.7 (99.7)	99.9 (100.0)	100.0 (99.9)
Multiplicity	6.7 (6.3)	3.8 (3.9)	6.8 (6.8)
Anomalous completeness (%)			99.9 (99.7)
Anomalous multiplicity			3.7 (3.6)
Refinement			
Maximum resolution used (Å)	2.58	2.05	
Number of reflections	39,120	25,227	
R-factor (%)	22.9	19.0	
Free *R*-factor (%)	26.5	22.4	
r.m.s.d. bond lengths (Å)	0.014	0.008	
r.m.s.d. bond angles (°)	1.520	0.940	
PDB accession code	3ZKJ	2WZK	
Average *B*-factor (Å^2)			
Chain A	59.97	34.37	
Chain B	89.76		
Chain C	123.24		
Chain D	68.45		
Chain E	97.14		
Chain F	89.11		
Waters	58.52	43.97	

Numbers in parentheses refer to the highest-resolution shell.

solved by molecular replacement and refined at 2.6 Å resolution (Fig. 1a; see Table 1 for data collection and refinement statistics). Six protein chains forming two ternary complexes were identified in the asymmetric unit (Supplementary Information, Fig. S1a). The two complexes were essentially identical except for a subtle shift in the relative position of the ankyrin domain with respect to the SOCS box (Supplementary Information, Fig. S1b) and some poor electron density in parts of Elongin B (chain C). Both regions were involved in crystal packing (Supplementary Information, Fig. S1a and c). Here, we focus our discussion on the ternary complex formed by chains D–F.

The ASB9–Elongin B/C complex adopts an elongated structure with overall dimensions of 110 Å × 45 Å × 40 Å (Fig. 1a and b). The ankyrin repeat domain sits atop the SOCS box and closely resembles the crescent-shape structures of other ankyrin proteins, including the ASB9-2 splice variant that lacks the SOCS box (r.m.s.d. of 1.3 Å over 218 C^{α} atoms). The consensus ankyrin repeat is a 33-residue motif that folds into a helix–loop–helix–β-hairpin structure [26,27]. In total, ASB9 contains seven tandem repeats, including six consensus repeats and a C-terminal capping repeat (Fig. 1a and c). The shorter capping repeat (Fig. 1a, inset) starts with an atypical 3_{10}-helix and connects to the C-terminal SOCS box, which binds Elongin B/C in a manner similar to other SOCS box E3 ligases. Notably, there is little interaction between the capping repeat and the SOCS box leaving a solvent-exposed channel through the ASB9 structure (Fig. 1b).

Ankyrin domains typically mediate protein–protein interactions through a binding groove on their concave inner face, which comprises the inner shorter α-helices and the β-hairpin regions [26,27]. This surface in ASB9 is also supported as the substrate-binding site by site-directed mutagenesis (Fig. 1b) [25]. Significantly for its E3 function, this surface is stably positioned to face the E2-ubiquitin moiety similar to the SOCS box structures of SOCS2 [28], SOCS4 [29], Gustavus [30], and VHL [31].

Interactions of the SOCS box

The SOCS box is a conserved three-helix motif (H1–H3) that facilitates multiple protein–protein interactions through its BC and Cullin box regions (Fig. 2a). The ASB9–Elongin B/C structure is the first to describe how the SOCS box assembles with the ankyrin repeat substrate-recognition domain. Comparison with other SOCS box structures reveals a three-residue insertion preceding the H2 helix of ASB9 that extends the SOCS box-ankyrin interface from repeats 4 to 6 (Fig. 2a). While the shorter inner helices of the ankyrin domain contribute to the

substrate-binding groove (Fig. 1a and b), the outer helices α8, α10, and α12 contribute to the SOCS box interaction (Fig. 2b). Of the three SOCS box insertion residues, Ile272 and Gln273 contact the ankyrin domain and form hydrophobic interactions with Ile154 and Ile160 as well as hydrogen bond interactions with Asn151 and Ser189, respectively.

ASB9 assembles with the Elongin B/C complex in a conserved manner through the amphipathic H1 helix of the SOCS box. The hydrophobic face includes the strictly conserved residues Leu258 and Cys262, which insert into the deep cleft between Elongin C loop 5 and H4 (Fig. 3a). Significant hydrophobic and main-chain hydrogen bond interactions are also made by ASB9 Pro255 and Pro256 to Elongin C H3 (Fig. 3a). The interactions of Elongin B are well described [28,31]. The long C-terminal tail extends from the base of the complex to occupy a hydrophobic pocket formed between Elongin C H4 and SOCS box helices H1 and H2. Here, the most significant contacts are made by Elongin B Pro100, Val102, and Met103 (Fig. 3b).

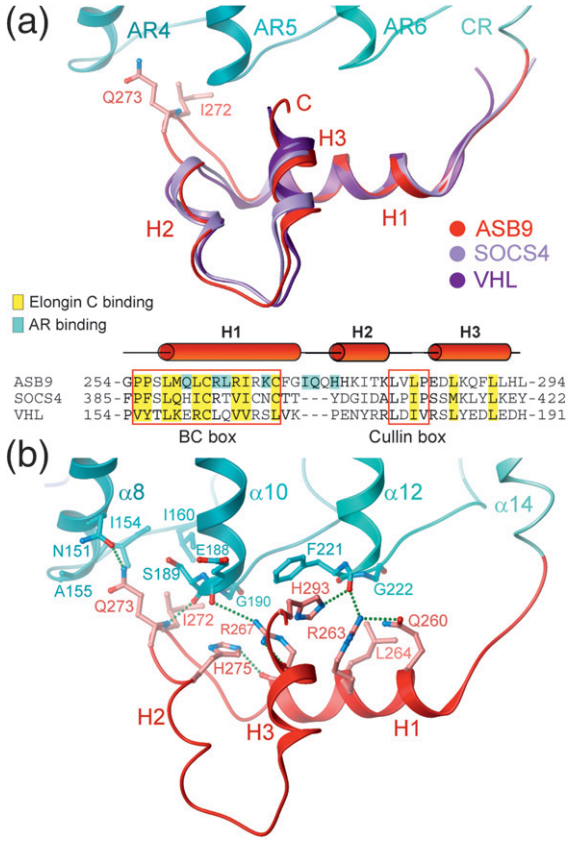

Fig. 2. SOCS box interactions with the ankyrin repeat domain. (a) Superposition of the SOCS box domains of ASB9, SOCS4 (PDB ID: 2IZV) [29], and VHL (PDB ID: 1VCB) [31] reveals a three-residue insertion in ASB9, which enables the SOCS box residues Ile172 and Gln273 to contact AR4 and AR5. The structure-based sequence alignment highlights SOCS box residues that contact the ankyrin domain (cyan) as well as those that bind Elongin C (yellow). The conserved BC box and Cullin box sequence motifs are boxed. (b) Side-chain interactions in the ankyrin–SOCS box interface. Hydrogen bonds are shown by a green broken line.

Structure of the Cul5 NTD

The SOCS box orchestrates the further assembly of the ASB9–Elongin B/C complex into Cul5-containing Cullin–RING complexes. Attempts to co-crystallize the higher-order Cul5 complex were unsuccessful. Since the structure of the Cul5 CTD was solved previously together with Rbx1 and Nedd8 [5], we tried instead to crystallize the missing N-terminal Cullin repeats. Viable crystals were obtained in space group $P2_12_12_1$ using a construct ($Cul5^{NTD}$) comprising residues 1 to 384 of mouse Cul5 and seven C-terminal residues remaining after tag cleavage. A molecular replacement solution could not be identified. Selenomethionine-incorporated protein crystals were therefore prepared and the structure was determined at 2.05 Å resolution using phases calculated from single-wavelength anomalous diffraction.

Overall, the $Cul5^{NTD}$ adopts an extended stalk-like structure similar to other Cullin family proteins (Fig. 4a). The NTD is composed of three consecutive Cullin repeat domains that are closely matched in structure (Fig. 4b). As observed for other Cullins, the five-helix fold is diverged in the first repeat, where the short H5 helix forms an insertion preceding the final helix (Fig. 4a). A further eight residues in the H5–H6 loop of the $Cul5^{NTD}$ were not defined by the electron density. Most significantly, the H5 helix is positioned seven residues further downstream than predicted by previous sequence alignments [7,12]. Misalignment potentially arose from a 25-residue insertion in the Cul1 H2–H3 loop, which is absent in Cul5 and disordered in the Cul1 structure (Supplementary Information, Fig. S2) [7]. Comparison of the $Cul5^{NTD}$ and other Cullin structures reveals significant deviations in the relative orientations of the three Cullin repeat domains (Fig. 4c). Most divergent are the Cul5 and Cul3 [32,35] structures that differ by a rotation of 28° between Cullin repeats 1 and 3 (Supplementary Information, Fig. S3). Such changes may reflect inherent flexibility in the Cullin scaffold and help to confer the correct geometry in each E3 for efficient ubiquitylation.

Cul5 assembly with ASB9–Elongin B/C

ASB9 contains a Cullin box sequence motif (281-Leu-Val-Leu-Pro-284; Fig. 2a) [12,13] that determines Cul5 interaction together with Elongin C [12,13,18,19]. We established a model for this assembly by superposition of the Elongin C and

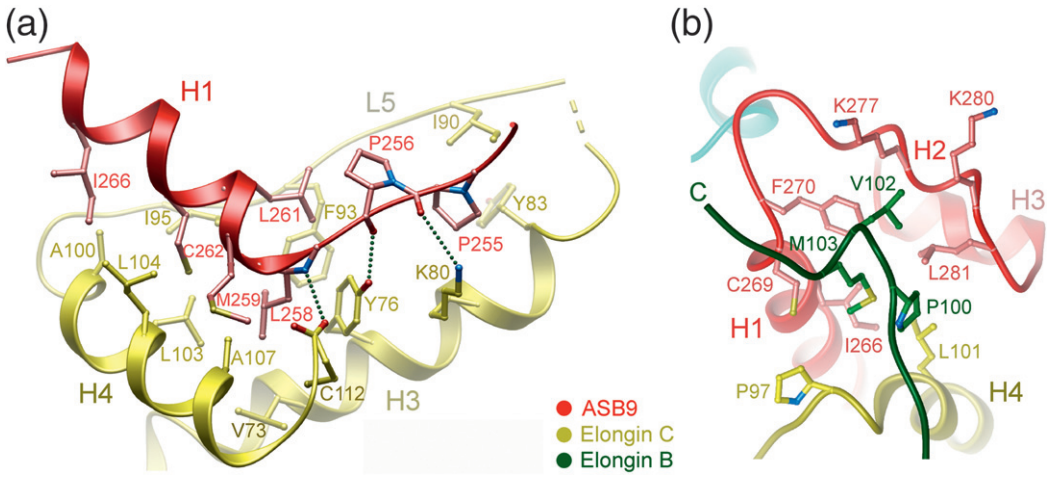

Fig. 3. SOCS box interactions with Elongin B/C. (a) Ribbon diagram of the ASB9–Elongin C interface showing the side-chain interactions of the BC box. (b) The C-terminal tail of Elongin B binds a hydrophobic pocket in the SOCS box.

Cul5^{NTD} subunits onto the Skp1–Cul1 structure [Protein Data Bank (PDB) ID: 1LDK] [7] and relaxed interface side chains using ICM-Pro (Fig. 5) [36]. The complexes center upon the Cullin H2 helix with additional contact from the short H5 [7]. While Cul1 depends on many tyrosine-mediated hydrogen-bonding interactions, the Cul5 interface is more hydrophobic (Fig. 5). In particular, the H2 helix presents an extended hydrophobic surface composed of Phe41, Phe44, His48, and Leu52. Binding experiments performed using surface plasmon resonance revealed a 50-fold loss in affinity for the mutants Phe41Ala and His48Ala and a complete loss of binding for Phe44Ala, as well as the neighboring Elongin C mutant Phe109Ala (Fig. 6). More peripheral substitutions were better tolerated. Predicted Cullin box interactions with Cul5 Leu52 were disrupted by the bulky substitution Leu52Tyr, but not by the alanine mutant Leu52Ala (Fig. 6). Similarly, the Gln113Ala mutation in the Cul5 H5 helix was well tolerated, with no apparent change in the binding affinity (Fig. 6). All of the mutants were highly expressed and showed the same elution profile on gel filtration as the wild-type protein, suggestive of proper folding.

To extend the model to the complete E3, we mapped onto the Cul5^{NTD} structure the neddylated Cul5^{CTD}–Rbx1 complex (PDB ID: 3DQV) [5] using the full-length Cul1 structure as a template (PDB ID: 1LDK) [7]. An E2-ubiquitin intermediate was modeled from the RNF4-UbcH5A-ubiquitin structure (PDB ID: 4AP4) [37] and docked onto Rbx1 by the homology of the RING domains. The final model orientates the substrate-binding groove of ASB9 towards the E2-ubiquitin with a distance of 100 Å to the reactive thioester bond (Fig. 7a). The substrate creatine

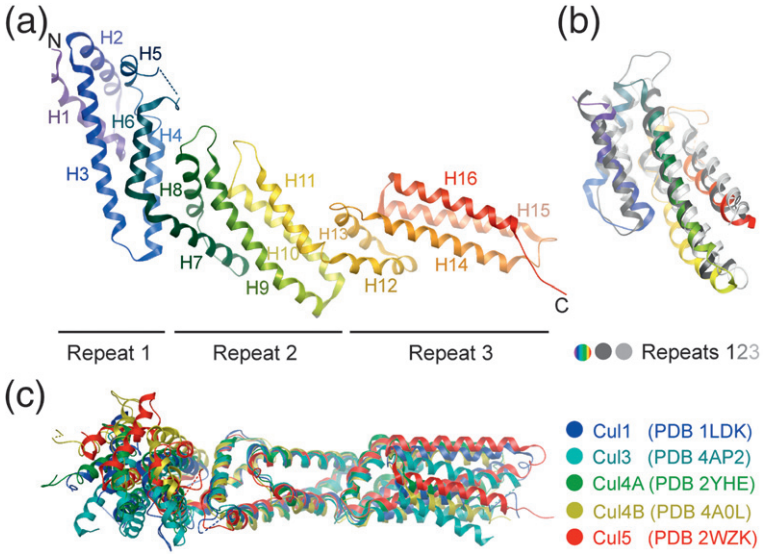

Fig. 4. Structure of the Cul5^{NTD}. (a) Ribbon diagram of the three Cullin repeat domains. Secondary-structure elements are labeled. (b) Superposition of repeats 1 to 3 shows the conserved Cullin fold. (c) The five known Cullin structures [7,32–34] are superimposed by the second Cullin repeat domain. Superposition reveals the rigid-body rotations between domains, with the largest deviations between repeats 1 and 2. Further comparisons with the Cul5^{NTD} structure are provided in Supplementary Information (Fig. S3).

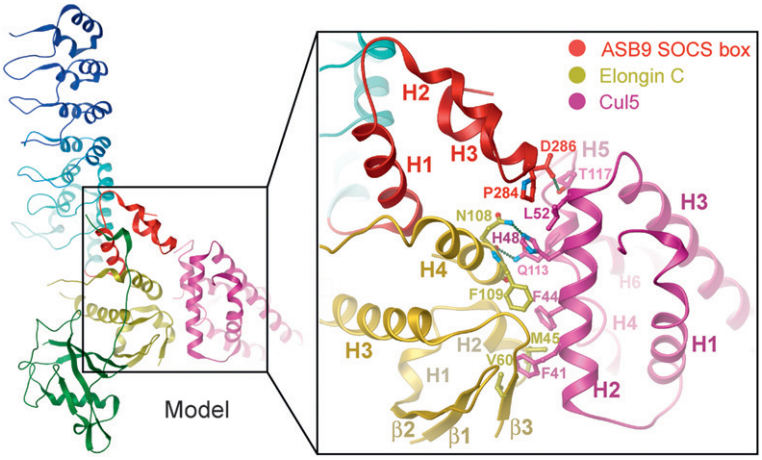

Fig. 5. Model for Cul5 assembly with the ASB9–Elongin B/C complex. The ASB9–Elongin B/C and Cul5^{NTD} structures were aligned to the Skp1–Cul1 template (PDB ID: 1LDK) [7] by superposition of the Elongin C and Cul5 subunits with the homologous Skp1 and Cul1, respectively. Inset displays side-chain interactions in the model (Elongin B is omitted for clarity).

kinase B has a diameter of 45 Å as a monomer but is known to dimerize, potentially reducing this gap further. For comparison, similar models were built for the prototypical SCF-type E3s with leucine-rich repeat (Fig. 7b) and WD40 repeat domains (Fig. 7c). Notably, these substrate-recognition domains adopt a perpendicular position to the ASB9 ankyrin domain, which further closes the gap to the E2-ubiquitin (82 Å and 65 Å, respectively). These distances are likely to be bridged by the remaining (non-crystallized) substrate regions as well as by the flexible association of the Rbx1 subunit with the neddylated Cullin.

Discussion

The SOCS box is a highly versatile motif that folds stably with a wide variety of E3 substrate-recognition domains. Here, we determined the molecular architecture of the ASB family, which uses an ankyrin repeat domain for substrate recognition. Remarkably for a 40-residue motif, the SOCS box establishes protein–protein interactions with four distinct domains, including the ankyrin domain, Elongin B, Elongin C, and Cul5. The ankyrin domain interaction is facilitated by an H1–H2 loop insertion that forms the primary adaptation of the ASB family. This positions the crescent shape of the ankyrin repeat domain roughly coaxial to the long axis of the Elongin B/C–SOCS box complex.

To date, Cullin–RING E3 ligase structures have shown the substrate-recognition domain extending out from the F-box or SOCS box in an L-shaped arrangement towards the RING-E2 subunits [3,4]. The structure of the ASB9–Elongin B/C ternary complex is the first to include the ankyrin domain and reveals a novel perpendicular packing arrangement. This alternative architecture appears favorable to present the substrate-binding site to the E2-ubiquitin. In addition, this arrangement creates a suitably wide spacing for large globular substrates, such as the creatine kinases. Whereas ASB proteins represent the most abundant SOCS box family, the ankyrin repeat domain is notably absent from the mammalian F-box class [41]. The Poxvirus F-box ankyrins, which hijack the mammalian ubiquitin–proteasome system, are a notable exception [42,43]. It will be interesting to determine whether these pack similarly to the SCF-type E3s or adopt the perpendicular arrangement of ASB9. The use of repeat domain proteins in Cullin–RING E3 ligases appears particularly common, from the Cullin repeats to the leucine-rich repeat, WD40 repeat, and ankyrin repeats of the substrate-recognition domain. Such proteins likely provide a highly advantageous scaffold to evolve a large repertoire of binders, perhaps explaining their enrichment.

The presented structure of the Cul5^{NTD} complements previous work on the Cul5^{CTD} and allows a model to be built for a complete Cul5-based E3 ligase [5]. Unexpectedly, the structure also exposes deviations to previous homology models, including rigid-body rotations and a change to the Cullin repeat sequence alignment. Rigid-body rotations between Cullin repeats have also been identified in different crystallized Cul1, Cul3, and Cul4 complexes, suggesting that the Cullin scaffold may also offer some flexibility to increase the catchment area for substrate and E2 or to provide alternative geometries for polyubiquitylation [32–34,44,45]. Although we present a model for the "monomeric" Cullin–RING E3 ligase complex, higher-order assemblies may also be possible. For example, non-canonical Cul1–Cul5 complexes are reported for ASB2 [46]. While no significant crystal contacts are present in the Cul5^{NTD} structure, some close packing is observed between neighboring Elongin B subunits, perhaps consistent with transient assemblies (Supplementary Information, Fig. S1c). Finally, dimerization of the RING domain may play a critical role in the ubiquitin transfer reaction [37,47,48].

The elucidation of the first structure of an ankyrin-containing Cullin–RING ligase reveals a

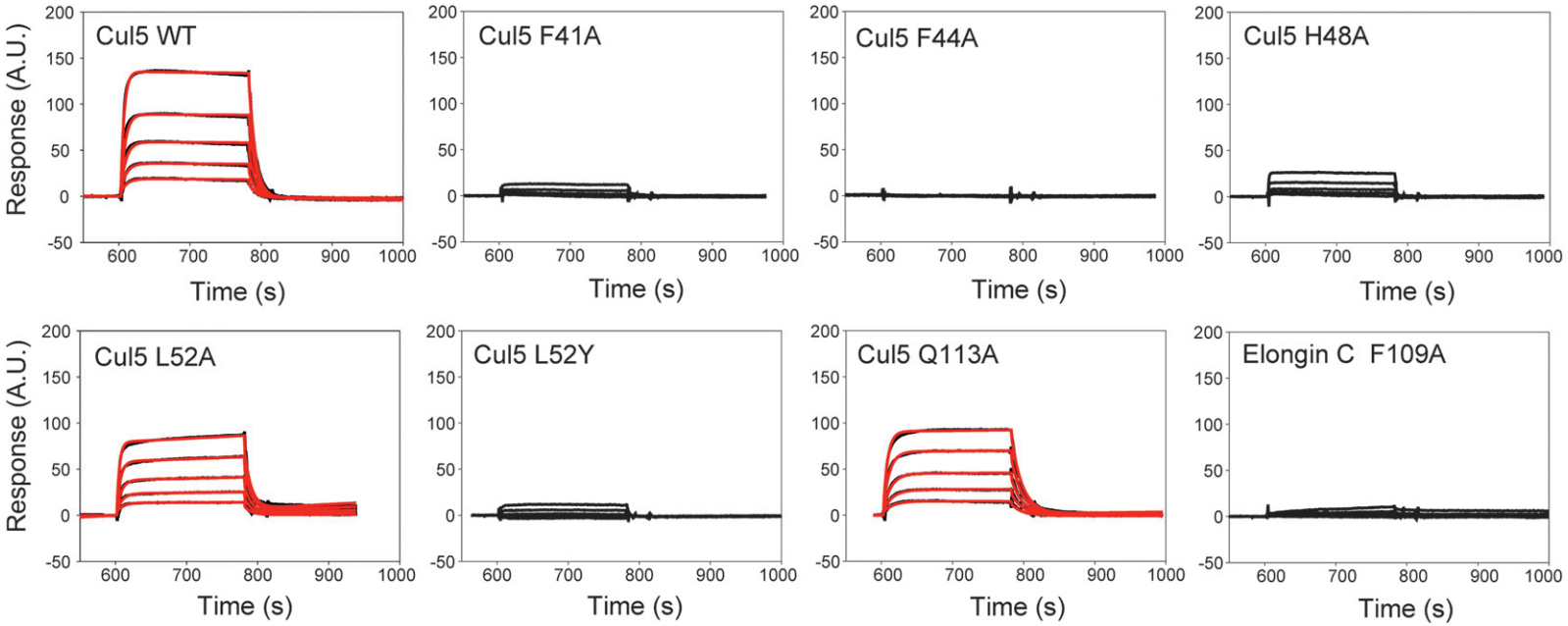

Cul5	ASB9-Elongin B/C	*ka* ($M^{-1} s^{-1}$)	*kd* (s^{-1})	K_D (μM)	χ^2
WT	WT	9.3×10^4	0.10	1.14	1.05
F41A	WT			>50	
F44A	WT			No binding	
H48A	WT			>50	
L52A	WT	8.7×10^4	0.10	1.23	1.1
L52Y	WT			>50	
Q113A	WT	5.0×10^4	0.06	1.31	0.6
WT	Elongin C F109C			No binding	

Fig. 6. Characterization of Cul5 binding. The ASB9–Elongin B/C complex was assayed for binding to immobilized GST-$Cul5^{NTD}$ using the Biacore 2000 platform (GE Healthcare). Wild-type and mutant complexes were analyzed at five different concentrations (2, 1, 0.5, 0.25, and 0.125 μM, black curves). Excellent fits to a 1:1 Langmuir binding model (red curves) were obtained for wild-type Cul5 and the Cul5 mutants Leu52Ala and Gln113Ala. The binding of other mutants was severely reduced. Kinetic parameters are given below the raw data. The values of the χ^2-statistical test indicate that the derived kinetic parameters are in good agreement with the raw data.

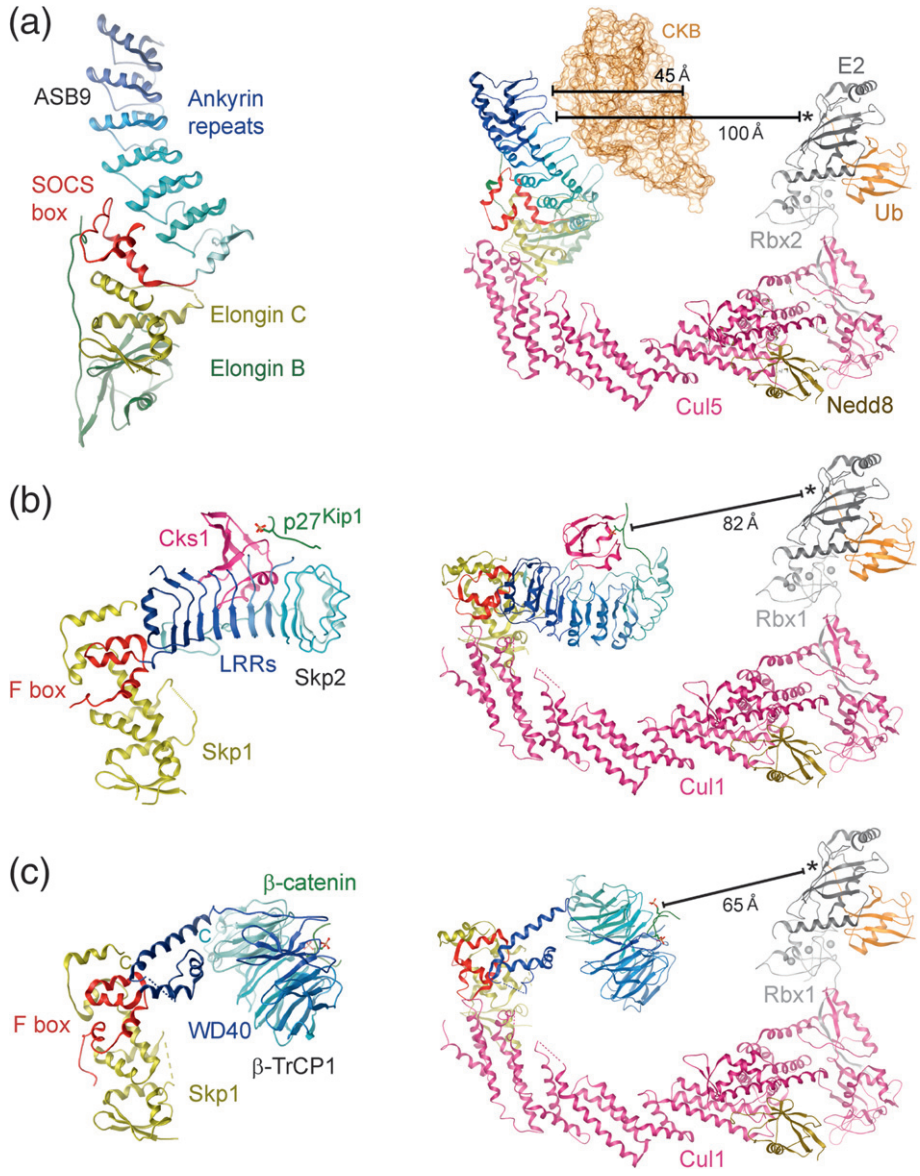

Fig. 7. Comparison of ankyrin repeat, leucine-rich repeat, and WD40 repeat domains. (a) Structure of the ASB9–Elongin B/C complex (left) and model for the complete E3 assembly (right). The neddylated $Cul5^{CTD}$–Rbx1 structure (PDB ID: 3DQV) [5] was built onto the $Cul5^{NTD}$ by superposition on the Cul1 template (PDB ID: 1LDK) [7]. An E2-ubiquitin intermediate was modeled from the RNF4-UbcH5A-ubiquitin structure (PDB ID: 4AP4) [37] by superposition of Rbx1 and RNF4. The final model orients the substrate-binding groove of ASB9 towards the E2-ubiquitin with a distance of 100 Å to the reactive thioester bond (marked by an asterisk). An outline molecular surface of a monomer of human creatine kinase B (orange, PDB ID: 3DRB) [38] is shown as a reference for the substrate position based on previous modeling [25]. (b) Comparable structure of the prototypical SCF-type E3 containing Skp1–Skp2–Cks1 bound to the substrate $p27^{Kip1}$ (PDB ID: 2AST) [39] (left) and model for the complete E3 assembly (right). The orientation shown is the same as the ASB9 complex based on the structural homology between Skp1 and Elongin C. The Skp2 leucine-rich repeat (LRR) domain is arranged perpendicularly to the ankyrin repeat domain of ASB9. Note the F-box occurs N-terminal to the LRR domain in Skp2, in contrast to the C-terminal SOCS box of ASB9. The substrate is positioned some 82 Å from the reactive thioester bond. (c) Structure of the Skp1–TrCP1 complex, which uses a WD40 repeat domain to recruit the substrate β-catenin (PDB ID: 1P22) [40] (left) and model for the complete E3 assembly (right). The substrate is positioned some 65 Å from the reactive thioester bond.

novel architecture for the E3 and further exemplifies the diversity of substrate recognition. This work provides a framework for understanding ASB-mediated ubiquitylation, as well as a Cul5 model to explore the interactions of other SOCS box families, including HIV Vif.

Materials and Methods

Plasmids

Human ASB9 (UniProt accession number Q96DX5, residues 35 to 294) and murine Cullin5 (Cul5^{NTD}; UniProt accession number Q9D5V5, residues 1–384) were subcloned into the vector pNIC-CTHF, which provides C-terminal hexahistidine and Flag tags cleavable by tobacco etch virus protease A [49]. Human Elongin B (UniProt accession number Q15370) and Elongin C (UniProt accession number Q15369, residues 17–112) were subcloned into pACYCDUET for co-expression with ASB9, as described previously [28]. For Biacore studies, a GST-Cul5^{NTD} construct was prepared in pGEX-4T. Mutants were constructed using the QuikChange Mutagenesis Kit (Stratagene) according to the manufacturer's instructions. All Cullin5 constructs were engineered according to the split and express strategy [50] to contain the solubilizing mutations Val341Arg and Leu345Asp.

Protein expression and purification

The human ASB9 protein was co-expressed with Elongin B/C in BL21(DE3) cells using 0.1 mM IPTG for overnight induction at 18 °C. Harvested cells were resuspended in binding buffer (50 mM Hepes, pH 7.5, 500 mM NaCl, 5% glycerol, and 30 mM imidazole) and disrupted by sonication. The ternary complex was purified by Ni-affinity and size-exclusion chromatography using a Superdex 200 HiLoad 16/60 column (GE Healthcare). Tobacco etch virus protease A was used to cleave the C-terminal tag. Further, Ni-affinity chromatography was used as a final polishing step to remove any remaining contaminants. For crystallization, the Cul5^{NTD} protein was expressed in BL21(DE3)-R3-pRARE cells and purified similarly. For selenomethionine labeling, Cul5^{NTD} was expressed in B834(DE3) supplemented with 40 mg/L L-selenomethionine. For Biacore studies, GST-Cul5^{NTD} was expressed in BL21(DE3) cells and purified on glutathione-Sepharose resin in phosphate-buffered saline containing 5 mM DTT and 1 mM PMSF. The protein was eluted in 100 mM Tris–HCl, pH 8.0, and 20 mM glutathione buffer and further purified by size-exclusion chromatography using a Superdex 200 26/60 column (GE Healthcare) equilibrated in 20 mM Hepes, 150 mM NaCl, and 2 mM DTT. Fractions were analyzed by SDS-PAGE and the purified protein was concentrated to 10 mg/mL.

Biosensor analysis

The ASB9–Elongin B/C interaction with murine Cul5 was investigated by biosensor analysis using the Biacore 2000 platform (GE Healthcare). Fifteen microliters of 10 μg/mL GST-Cul5^{NTD} was immobilized onto an anti-GST coated CM5 sensor chip (GE Healthcare) using a flow rate of 5 μL/min. Wild type and individual point mutants of Cul5 were each immobilized in this manner to a surface density of approximately 250 response units. Binding of the wild-type ASB9–Elongin B/C ternary complex to Cul5 was then analyzed by diluting the protein complex in Hepes-buffered saline containing 0.01% (v/v) Tween-20 and passing it over the chip at 20 μL/min. The complexes were analyzed at five different concentrations (2, 1, 0.5, 0.25, and 0.125 μM). An ASB9–Elongin B/C complex with a point mutation in Elongin C (F109A) was analyzed under identical conditions. The chip was regenerated by the addition of 10 mM glycine, pH 2.0, after each sample addition. Data were analyzed using the BIAEVALUATION software (GE Healthcare) and fitting to a 1:1 Langmuir binding model.

Structure determination of ASB9–Elongin B/C

Crystallization was achieved at 4 °C using the sitting-drop vapor diffusion method. The ASB9–Elongin B/C complex buffered in 50 mM Hepes, pH 7.5, 500 mM NaCl, and 10 mM DTT was concentrated to 40 mg/mL and crystallized using a precipitant containing 0.20 M Na(malonate), 0.1 M Bistris (2-[bis(2-hydroxyethyl)amino]-2-(hydroxymethyl)propane-1,3-diol) propane, pH 6.5, 20% polyethylene glycol 3350, and 10% ethylene glycol. Viable crystals were obtained from a 300-nL drop when the protein solution was mixed with the reservoir solution at a 2:1 volume ratio. Crystals were cryo-protected with mother liquor plus 10% ethylene glycol, prior to vitrification in liquid nitrogen. Crystals were tested at Diamond Light Source beamlines I02, I03, and I24, with final data collected at beamline I02 and processed using the CCP4 suite [51]. The ternary complex crystallized in the orthorhombic space group $P2_122_1$ with two molecules in the asymmetric unit. The structure was solved by molecular replacement using PHASER [52] and the structures of hASB9-2 (PDB ID: 3D9H) and Elongin B/C (PDB ID: 2C9W) as search models. Iterative cycles of restrained refinement and manual model building were performed using Coot [53] and PHENIX [54].

Structure determination of Cul5^{NTD}

Protein was concentrated to 16 mg/mL buffered in 50 mM Hepes, pH 7.5, 300 mM NaCl, 10 mM DTT, 0.5 mM TCEP, 10 mM L-arginine, and 10 mM L-glutamic acid. Native crystals were grown at 20 °C in 150-nL sitting drops mixing 50 nL of protein solution with 100 nL of a reservoir solution containing 0.1 M Bistris, pH 6.5, 25% polyethylene glycol 3350, and 0.15 M NH_4SO_2. Mounted crystals were cryo-protected with an additional 25% ethylene glycol. Crystals of the selenomethionine-labeled protein were grown at 20 °C in 150-nL sitting drops mixing 75 nL of protein solution with 75 nL of reservoir solution containing 20% Jeffamine ED-2001 reagent pH 7.0, and 0.1 M Hepes, pH 6.8. Crystals were cryo-protected with an additional 25% ethylene glycol. Diffraction data were collected at 100 K at Diamond Light Source, beamline I02 for native Cul5^{NTD} and beamline I03 for the selenomethionine-labeled crystal. Data were processed using MOSFLM [55] and scaled using SCALA from the CCP4 suite [51]. Phases were calculated using selenomethionine single-wavelength anomalous diffraction data and extended to the highest resolution with SOLVE [56]. An initial structural model was built using ARP/wARP [57]. Both Cul5^{NTD} proteins crystallized in the orthorhombic space group $P2_12_12_1$ with one molecule in the asymmetric unit. Iterative cycles of restrained refinement and manual model

building were performed using Coot [53], REFMAC5 [58], and PHENIX [54].

Accession numbers

The atomic coordinates and structure factors have been deposited in the PDB with the following accession numbers: PDB ID: 3ZKJ and PDB ID: 2WZK.

Acknowledgements

The authors would like to thank Diamond Light Source and the staff of beamlines I02, I03, and I24 (proposal mx442) for access and assistance with crystal testing and data collection and Peter Canning for artwork. The SGC is a registered charity (number 1097737) that receives funds from AbbVie, Boehringer Ingelheim, the Canada Foundation for Innovation, the Canadian Institutes of Health Research, Genome Canada, GlaxoSmithKline, Janssen, Lilly Canada, the Novartis Research Foundation, the Ontario Ministry of Economic Development and Innovation, Pfizer, Takeda, and the Wellcome Trust (092809/Z/10/Z). This work was supported in part by the National Health and Medical Research Council of Australia (NHMRC) project grant 1011804, the Victorian State Government Operational Infrastructure Support grant, and the NHMRC Independent Research Institutes Infrastructure Support Scheme (361646). J.J.B. acknowledges support from the Australian Research Council.

Supplementary Data

Supplementary data to this article can be found online at http://dx.doi.org/10.1016/j.jmb.2013.06.015

Received 28 April 2013;
Received in revised form 10 June 2013;
Accepted 11 June 2013
Available online 25 June 2013

Keywords:
proteasome;
signaling;
ubiquitination;
degradation;
protein–protein interaction

Present address: J.R.C. Muniz, Institute of Physics of São Carlos, University of São Paulo, Avenida Trabalhador Sãocarlense 400, São Carlos, SP 13560-970, Brazil.

Abbreviations used:
NTD, N-terminal domain; CTD, C-terminal domain; PDB, Protein Data Bank; SOCS, suppressor of cytokine signaling; SCF, Skp1–Cul1–F-box; ASB, ankyrin SOCS box.

References

[1] Schulman BA, Harper JW. Ubiquitin-like protein activation by E1 enzymes: the apex for downstream signalling pathways. Nat Rev Mol Cell Biol 2009;10:319–31.
[2] Hershko A, Ciechanover A. The ubiquitin system. Annu Rev Biochem 1998;67:425–79.
[3] Petroski MD, Deshaies RJ. Function and regulation of cullin-RING ubiquitin ligases. Nat Rev Mol Cell Biol 2005;6:9–20.
[4] Zimmerman ES, Schulman BA, Zheng N. Structural assembly of cullin-RING ubiquitin ligase complexes. Curr Opin Struct Biol 2010;20:714–21.
[5] Duda DM, Borg LA, Scott DC, Hunt HW, Hammel M, Schulman BA. Structural insights into NEDD8 activation of cullin-RING ligases: conformational control of conjugation. Cell 2008;134:995–1006.
[6] Saha A, Deshaies RJ. Multimodal activation of the ubiquitin ligase SCF by Nedd8 conjugation. Mol Cell 2008;32:21–31.
[7] Zheng N, Schulman BA, Song L, Miller JJ, Jeffrey PD, Wang P, et al. Structure of the Cul1–Rbx1–Skp1–F boxSkp2 SCF ubiquitin ligase complex. Nature 2002;416:703–9.
[8] Kile BT, Schulman BA, Alexander WS, Nicola NA, Martin HM, Hilton DJ. The SOCS box: a tale of destruction and degradation. Trends Biochem Sci 2002;27:235–41.
[9] Linossi EM, Nicholson SE. The SOCS box-adapting proteins for ubiquitination and proteasomal degradation. IUBMB Life 2012;64:316–23.
[10] Hilton DJ, Richardson RT, Alexander WS, Viney EM, Willson TA, Sprigg NS, et al. Twenty proteins containing a C-terminal SOCS box form five structural classes. Proc Natl Acad Sci USA 1998;95:114–9.
[11] Kamura T, Sato S, Haque D, Liu L, Kaelin Jr WG, Conaway RC, et al. The Elongin BC complex interacts with the conserved SOCS-box motif present in members of the SOCS, ras, WD-40 repeat, and ankyrin repeat families. Genes Dev 1998;12:3872–81.
[12] Kamura T, Maenaka K, Kotoshiba S, Matsumoto M, Kohda D, Conaway RC, et al. VHL-box and SOCS-box domains determine binding specificity for Cul2–Rbx1 and Cul5–Rbx2 modules of ubiquitin ligases. Genes Dev 2004;18:3055–65.
[13] Mahrour N, Redwine WB, Florens L, Swanson SK, Martin-Brown S, Bradford WD, et al. Characterization of Cullin-box sequences that direct recruitment of Cul2–Rbx1 and Cul5–Rbx2 modules to Elongin BC-based ubiquitin ligases. J Biol Chem 2008;283:8005–13.
[14] Heuze ML, Guibal FC, Banks CA, Conaway JW, Conaway RC, Cayre YE, et al. ASB2 is an Elongin BC-interacting protein that can assemble with Cullin 5 and Rbx1 to reconstitute an E3 ubiquitin ligase complex. J Biol Chem 2005;280:5468–74.
[15] Kohroki J, Nishiyama T, Nakamura T, Masuho Y. ASB proteins interact with Cullin5 and Rbx2 to form E3 ubiquitin ligase complexes. FEBS Lett 2005;579:6796–802.
[16] Wang J, Muntean AG, Hess JL. ECSASB2 mediates MLL degradation during hematopoietic differentiation. Blood 2012;119:1151–61.
[17] Heuze ML, Lamsoul I, Baldassarre M, Lad Y, Leveque S, Razinia Z, et al. ASB2 targets filamins A and B to proteasomal degradation. Blood 2008;112:5130–40.

[18] Kwon S, Kim D, Rhee JW, Park JA, Kim DW, Kim DS, et al. ASB9 interacts with ubiquitous mitochondrial creatine kinase and inhibits mitochondrial function. BMC Biol 2010;8:23.
[19] Debrincat MA, Zhang JG, Willson TA, Silke J, Connolly LM, Simpson RJ, et al. Ankyrin repeat and suppressors of cytokine signaling box protein asb-9 targets creatine kinase B for degradation. J Biol Chem 2007;282:4728–37.
[20] Tokuoka M, Miyoshi N, Hitora T, Mimori K, Tanaka F, Shibata K, et al. Clinical significance of ASB9 in human colorectal cancer. Int J Oncol 2010;37:1105–11.
[21] Chung AS, Guan YJ, Yuan ZL, Albina JE, Chin YE. Ankyrin repeat and SOCS box 3 (ASB3) mediates ubiquitination and degradation of tumor necrosis factor receptor II. Mol Cell Biol 2005;25:4716–26.
[22] Li JY, Chai B, Zhang W, Wu X, Zhang C, Fritze D, et al. Ankyrin repeat and SOCS box containing protein 4 (Asb-4) colocalizes with insulin receptor substrate 4 (IRS4) in the hypothalamic neurons and mediates IRS4 degradation. BMC Neurosci 2011;12:95.
[23] Diks SH, Sartori da Silva MA, Hillebrands JL, Bink RJ, Versteeg HH, van Rooijen C, et al. d-Asb11 is an essential mediator of canonical Delta-Notch signalling. Nat Cell Biol 2008;10:1190–8.
[24] Sartori da Silva MA, Tee JM, Paridaen J, Brouwers A, Runtuwene V, Zivkovic D, et al. Essential role for the d-Asb11 cul5 Box domain for proper notch signaling and neural cell fate decisions in vivo. PLoS One 2010;5:e14023.
[25] Fei X, Gu X, Fan S, Yang Z, Li F, Zhang C, et al. Crystal structure of Human ASB9-2 and substrate-recognition of CKB. Protein J 2012;31:275–84.
[26] Mosavi LK, Minor Jr DL, Peng ZY. Consensus-derived structural determinants of the ankyrin repeat motif. Proc Natl Acad Sci USA 2002;99:16029–34.
[27] Sedgwick SG, Smerdon SJ. The ankyrin repeat: a diversity of interactions on a common structural framework. Trends Biochem Sci 1999;24:311–6.
[28] Bullock AN, Debreczeni JE, Edwards AM, Sundstrom M, Knapp S. Crystal structure of the SOCS2–elongin C–elongin B complex defines a prototypical SOCS box ubiquitin ligase. Proc Natl Acad Sci USA 2006;103:7637–42.
[29] Bullock AN, Rodriguez MC, Debreczeni JE, Songyang Z, Knapp S. Structure of the SOCS4-ElonginB/C complex reveals a distinct SOCS box interface and the molecular basis for SOCS-dependent EGFR degradation. Structure 2007;15:1493–504.
[30] Woo JS, Imm JH, Min CK, Kim KJ, Cha SS, Oh BH. Structural and functional insights into the B30.2/SPRY domain. EMBO J 2006;25:1353–63.
[31] Stebbins CE, Kaelin Jr WG, Pavletich NP. Structure of the VHL–ElonginC–ElonginB complex: implications for VHL tumor suppressor function. Science 1999;284:455–61.
[32] Canning P, Cooper CD, Krojer T, Murray JW, Pike AC, Chaikuad A, et al. Structural basis for Cul3 assembly with the BTB-Kelch family of E3 ubiquitin ligases. J Biol Chem 2013;288:7803–14.
[33] Fischer ES, Scrima A, Bohm K, Matsumoto S, Lingaraju GM, Faty M, et al. The molecular basis of CRL4DDB2/CSA ubiquitin ligase architecture, targeting, and activation. Cell 2011;147:1024–39.
[34] Angers S, Li T, Yi X, MacCoss MJ, Moon RT, Zheng N. Molecular architecture and assembly of the DDB1-CUL4A ubiquitin ligase machinery. Nature 2006;443:590–3.
[35] Ji AX, Prive GG. Crystal structure of KLHL3 in complex with Cullin3. PLoS One 2013;8:e60445.
[36] Abagyan RA, Totrov M, Kuznetsov D. ICM: a new method for protein modeling and design: applications to docking and structure prediction from the distorted native conformation. J Comput Chem 1994;15:488–506.
[37] Plechanovova A, Jaffray EG, Tatham MH, Naismith JH, Hay RT. Structure of a RING E3 ligase and ubiquitin-loaded E2 primed for catalysis. Nature 2012;489:115–20.
[38] Bong SM, Moon JH, Nam KH, Lee KS, Chi YM, Hwang KY. Structural studies of human brain-type creatine kinase complexed with the ADP–Mg_2^+–NO_3^-–creatine transition-state analogue complex. FEBS Lett 2008;582:3959–65.
[39] Hao B, Zheng N, Schulman BA, Wu G, Miller JJ, Pagano M, et al. Structural basis of the Cks1-dependent recognition of p27(Kip1) by the SCF(Skp2) ubiquitin ligase. Mol Cell 2005;20:9–19.
[40] Wu G, Xu G, Schulman BA, Jeffrey PD, Harper JW, Pavletich NP. Structure of a beta-TrCP1–Skp1–beta-catenin complex: destruction motif binding and lysine specificity of the SCF(beta-TrCP1) ubiquitin ligase. Mol Cell 2003;11:1445–56.
[41] Jin J, Cardozo T, Lovering RC, Elledge SJ, Pagano M, Harper JW. Systematic analysis and nomenclature of mammalian F-box proteins. Genes Dev 2004;18:2573–80.
[42] Sonnberg S, Seet BT, Pawson T, Fleming SB, Mercer AA. Poxvirus ankyrin repeat proteins are a unique class of F-box proteins that associate with cellular SCF1 ubiquitin ligase complexes. Proc Natl Acad Sci USA 2008;105:10955–60.
[43] Barry M, van Buuren N, Burles K, Mottet K, Wang Q, Teale A. Poxvirus exploitation of the ubiquitin–proteasome system. Viruses 2010;2:2356–80.
[44] Liu J, Nussinov R. Flexible cullins in cullin-RING E3 ligases allosterically regulate ubiquitination. J Biol Chem 2011;286:40934–42.
[45] Zhuang M, Calabrese MF, Liu J, Waddell MB, Nourse A, Hammel M, et al. Structures of SPOP–substrate complexes: insights into molecular architectures of BTB-Cul3 ubiquitin ligases. Mol Cell 2009;36:39–50.
[46] Nie L, Zhao Y, Wu W, Yang YZ, Wang HC, Sun XH. Notch-induced Asb2 expression promotes protein ubiquitination by forming non-canonical E3 ligase complexes. Cell Res 2011;21:754–69.
[47] Dou H, Buetow L, Sibbet GJ, Cameron K, Huang DT. BIRC7-E2 ubiquitin conjugate structure reveals the mechanism of ubiquitin transfer by a RING dimer. Nat Struct Mol Biol 2012;19:876–83.
[48] Pruneda JN, Littlefield PJ, Soss SE, Nordquist KA, Chazin WJ, Brzovic PS, et al. Structure of an E3:E2 Ub complex reveals an allosteric mechanism shared among RING/U-box ligases. Mol Cell 2012;47:933–42.
[49] Savitsky P, Bray J, Cooper CD, Marsden BD, Mahajan P, Burgess-Brown NA, et al. High-throughput production of human proteins for crystallization: the SGC experience. J Struct Biol 2010;172:3–13.
[50] Li T, Pavletich NP, Schulman BA, Zheng N. High-level expression and purification of recombinant SCF ubiquitin ligases. Methods Enzymol 2005;398:125–42.
[51] Collaborative Computational Project Number 4. The CCP4 suite: programs for protein crystallography. Acta Crystallogr Sect D Biol Crystallogr 1994;50:760–3.
[52] McCoy AJ, Grosse-Kunstleve RW, Adams PD, Winn MD, Storoni LC, Read RJ. Phaser crystallographic software. J Appl Crystallogr 2007;40:658–74.

[53] Emsley P, Lohkamp B, Scott WG, Cowtan K. Features and development of Coot. Acta Crystallogr Sect D Biol Crystallogr 2010;66:486–501.
[54] Adams PD, Afonine PV, Bunkoczi G, Chen VB, Davis IW, Echols N, et al. PHENIX: a comprehensive Python-based system for macromolecular structure solution. Acta Crystallogr Sect D Biol Crystallogr 2010;66:213–21.
[55] Leslie AG. The integration of macromolecular diffraction data. Acta Crystallogr Sect D Biol Crystallogr 2006;62:48–57.
[56] Terwilliger TC, Berendzen J. Automated MAD and MIR structure solution. Acta Crystallogr Sect D Biol Crystallogr 1999;55:849–61.
[57] Perrakis A, Morris R, Lamzin VS. Automated protein model building combined with iterative structure refinement. Nat Struct Biol 1999;6:458–63.
[58] Murshudov GN, Vagin AA, Dodson EJ. Refinement of macromolecular structures by the maximum-likelihood method. Acta Crystallogr Sect D Biol Crystallogr 1997;53:240–55.